

Interface bonding of NiCrAlY coating on laser modified H13 tool steel surface

M. S. Reza¹ · S. N. Aqida^{1,2} · I. Ismail²

Received: 17 October 2015 / Accepted: 10 May 2016 / Published online: 24 May 2016
© Springer-Verlag Berlin Heidelberg 2016

Abstract Bonding strength of thermal spray coatings depends on the interfacial adhesion between bond coat and substrate material. In this paper, NiCrAlY (Ni-164/211 Ni22 %Cr10 %Al1.0 %Y) coatings were developed on laser modified H13 tool steel surface using atmospheric plasma spray (APS). Different laser peak power, P_p , and duty cycle, DC, were investigated in order to improve the mechanical properties of H13 tool steel surface. The APS spraying parameters setting for coatings were set constant. The coating microstructure near the interface was analyzed using IM7000 inverted optical microscope. Interface bonding of NiCrAlY was investigated by interfacial indentation test (IIT) method using MMT-X7 Matsuzawa Hardness Tester Machine with Vickers indenter. Diffusion of atoms along NiCrAlY coating, laser modified and substrate layers was investigated by energy-dispersive X-ray spectroscopy (EDXS) using Hitachi Tabletop Microscope TM3030 Plus. Based on IIT method results, average interfacial toughness, K_{avg} , for reference sample was $2.15 \text{ MPa m}^{1/2}$ compared to sample L1 range of K_{avg} from 6.02 to $6.96 \text{ MPa m}^{1/2}$ and sample L2 range of K_{avg} from 2.47 to $3.46 \text{ MPa m}^{1/2}$. Hence, according to K_{avg} , sample L1 has the highest interface bonding and is being laser modified at lower laser peak power, P_p , and higher duty cycle, DC, prior to coating. The EDXS analysis indicated the presence of Fe in the NiCrAlY coating layer and increased Ni and Cr composition in the laser modified

layer. Atomic diffusion occurred in both coating and laser modified layers involved in Fe, Ni and Cr elements. These findings introduce enhancement of coating system by substrate surface modification to allow atomic diffusion.

1 Introduction

H13 tool steel has been used as die steel material in semisolid forming processing. This process involves cyclic high-temperature metal injection, solidification and rapid quenching by water-based lubricants in the die. Rapid heating and cooling cause die surface to compress and tension, respectively, and lead to crack and fatigue failure. Hence, it is important to maintain die surface from damage and failure. In order to reduce damage at contact surface, many researches indicate surface treatment and coating are the most effective methods for die surface protection [1, 2]. To date, many research works have been conducted to enhance/harden metal surface through coatings and surface modification. Many difficulties were encountered to meet coating requirements such as excellent bonding, adequate thickness, suitable mechanical properties, thermal shock resistance and high temperature stability [3, 4]. Therefore, laser surface modifications are prior methods that can improve coating characteristics, especially thermal barrier coatings.

NiCrAlY alloys are excellent to resist oxidation and hot corrosion. It is frequently being used as bond coats for ceramic coating like yttria-stabilized zirconia (YSZ) to resist corrosion up to $980 \text{ }^\circ\text{C}$. Coating and its affect on adhesion to the substrate are closely linked to the coating microstructure, specifically Kirkendall voids, oxides and intermetallic compounds [5–7]. Alumina, Al_2O_3 , is the preferred oxide because of its low oxygen diffusivity and

✉ S. N. Aqida
aqida@ump.edu.my

¹ Faculty of Mechanical Engineering, University Malaysia Pahang, 26600 Pekan, Pahang, Malaysia

² Automotive Engineering Centre, Universiti Malaysia Pahang, 26600 Pekan, Pahang, Malaysia

superior adherence. But, formation of Al_2O_3 along with other oxides may be detrimental to the coating characteristics, especially adhesion.

During coating process, as the system cools to ambient temperature, alumina layer develops extremely large residual compressions. This is primarily because of misfit thermal expansion of coating material to the substrate. Stresses also arise during thermally grown oxide (TGO) formation, but they are much smaller (<1 GPa) [8]. When coating was applied by plasma spraying, substantial residual stress may be induced in the deposits, at the substrate–coating interface. These stresses originate from the differential contraction generated between the various materials because of their different physical and mechanical properties (Young's modulus, expansion coefficient, etc.).

This paper investigates adhesion of bond coat NiCrAlY on laser modified (LSM) AISI H13 tool steel substrate, its effects on fracture toughness and elements diffusion with the setup laser parameters indicated.

2 Methodology and materials

The material investigated in this study was AISI H13 tool steel being used for the experimental substrate. As received, 10 mm diameters with 150 mm length H13 tool steel cylindrical samples were cleaned with ethanol prior to processing. Two cylindrical samples, $L1$ and $L2$, are laser-modified on its circumferential surface and are coated with nickel-based alloy (NiCrAlY). One sample which was the reference sample was being coated with nickel-based alloy (NiCrAlY) without the laser modification prior to coating. Table 1 shows the chemical composition of AISI H13 tool steel material as the substrate material being coated with bond coat NiCrAlY.

A Rofin DC-015 diffusion-cooled CO_2 slab laser system with $10.6\ \mu\text{m}$ wavelength was used to modify the sample surface. The laser system was focused on a minimum laser spot diameter of $0.09\ \text{mm}$ onto sample surface and was

defocused above the surface to achieve a larger spot diameter of $0.2\ \text{mm}$. Table 2 indicates the parameter settings for laser surface modification. The parameters used were laser peak power, P_p , duty cycle, DC, and pulse repetition frequency, PRF. The duty cycle was based on laser power to result in average power of $274.2\ \text{W}$. The outcome parameters from the settings were residence time, T_R , and irradiance, I , which were calculated using Eqs. 1 and 2.

$$T_R = \frac{\text{DC} \times d}{S} \quad (1)$$

$$I = \frac{F}{T_R} \times \text{DC} \quad (2)$$

where d is laser spot diameter, F is energy density (pulse energy divided by laser beam spot area), and S is traverse speed (laser spot diameter divided by time taken to produce one rotation).

Atmospheric plasma spray method was used to deposit NiCrAlY coating. Praxair Ni-164/211 Ni22 %Cr10 %Al1.0 %Y alloy powders were deposited on laser modified surface samples at parameters settings shown in Table 3.

Metallographic study was carried out using IM7000 inverted optical microscope and is being analyzed by using image analysis software. Elements diffusion was investigated by energy-dispersive X-ray spectroscopy (EDXS) using Hitachi Tabletop Microscope TM3030 Plus. Energy-dispersive X-ray spectroscopy (EDXS) setup was employed with observation condition of $15\ \text{kV}$ accelerating voltage that was applied to the electron probe and spatial resolution setup with standard backscattered observation mode. Interfacial indentation test (IIT) was conducted using MMT-X7 Matsuzawa hardness test machine at 0.5 and $1.0\ \text{kg}$ load. The IIT was carried out at substrate/coating interface of polished cross-sectional surface. As shown in Fig. 1, indentation load was applied for a period of $10\ \text{s}$ to include delayed cracks. The adhesion was determined by measuring the length of the radial crack caused by the penetration of the Vickers diamond.

Table 1 Chemical composition, wt% of AISI H13 tool steel substrate and NiCrAlY coating powder

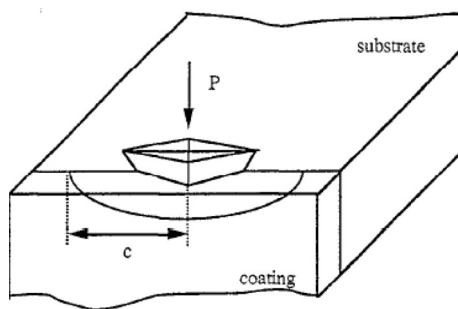
Material	C	Mn	Si	Cr	Ni	Mo	V	Cu	P	S	Fe
H13	0.32–0.45	0.20–0.50	0.80–1.20	4.75–5.50	0.30	1.10–1.75	0.80–1.20	0.25	0.03	0.03	Bal.
NiCrAlY	Ni	Cr	Al	Y							
	67.0	22.0	10.0	1.0							

Table 2 Laser surface modification of H13 steel parameter settings

Sample	P_p (W)	DC (%)	PRF (Hz)	Residence time, T_R (ms)	Irradiance, I (W/mm^2)
$L1$	760	36.1	2300	0.157	119,464.45
$L2$	1515	18.1	2300	0.0787	238,142.95

Table 3 Parameter settings for APS deposition of NiCrAlY coating

Parameters	Unit	APS setting for NiCrAlY
Feed rate	g/min	40
Secondary gas (He)	kPa	345
Primary gas (Ar)	kPa	345
Carrier gas (Ar)	kPa	345
Current	A	500
Stand-off distance	mm	110
No. of cycle	no.	L1 = 10; L2 = 9, reference sample = 10
Torch speed	%	40
Workpiece rotational speed	rpm	250

**Fig. 1** Principle of interfacial indentation test (IIT)

2.1 Interfacial toughness, K_C , calculation

The interfacial toughness, K_C , was referred to Chicot and Lesage et al. [9], where (P_c, a_c) couple was associated with the interfacial crack initiation as given in Eqs. 1 and 2.

$$K_C = 0.015 \frac{P_c}{a_c^{3/2}} \times \left(\frac{E}{H} \right)^{1/2} \quad (1)$$

where P_c is the applied critical load, and a_c is the interfacial crack length. The $(E/H)_I$ ratio, defined in Eq. (2), characterizes the global behavior of the coating/substrate system.

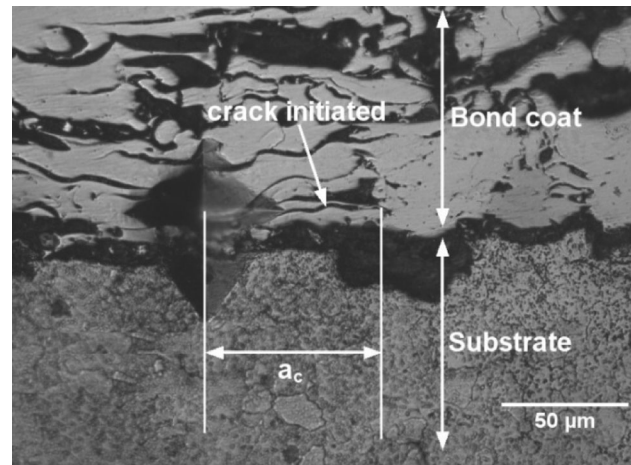
$$\left(\frac{E}{H} \right)^{1/2} = \frac{\left(\frac{E}{H} \right)_S^{1/2}}{1 + \left(\frac{H_S}{H_C} \right)} + \frac{\left(\frac{E}{H} \right)_C^{1/2}}{1 + \left(\frac{H_C}{H_S} \right)} \quad (2)$$

where E is the Young modulus, H is the hardness, and I, S and C subscripts stand for interface, substrate and coating, respectively.

3 Results and discussion

3.1 Interfacial toughness, K

Micrograph from interfacial indentation test of reference sample, AISI H13 tool steel, coated with NiCrAlY bond

**Fig. 2** Micrograph of reference sample cross section with indentation mark at NiCrAlY coating/H13 substrate interface

coat is shown in Fig. 2. A crack length of $69.14 \mu\text{m}$ and interfacial toughness $K_C = 2.08 \text{ MPa m}^{1/2}$ were measured at substrate–bond coat interface.

whereby micrograph for samples $L1$ and $L2$ from interfacial indentation test of NiCrAlY coating with laser modified layer is shown in Fig. 3. The crack length measured for sample $L1$ was $41.1 \mu\text{m}$ and sample $L2$ was $54.7 \mu\text{m}$, respectively. Crack initiated from the center of indentation mark and propagated along the NiCrAlY coating/laser modified surface interface.

Referring to Table 4, the average interfacial toughness, K_C , from IIT test results was $2.15 \text{ MPa m}^{1/2}$, relatively lower than average interfacial toughness obtained for samples $L1$ and $L2$ which are laser modified AISI H13 tool steel coated with NiCrAlY. Sample $L1$ indicates a higher interfacial toughness, K_{avg} , range of 6.02 to $6.96 \text{ MPa m}^{1/2}$ compared to sample $L2$ with K_{avg} range of 2.47 – $3.46 \text{ MPa m}^{1/2}$. Higher K_{avg} value was due to enhanced adhesion bonding between coating and laser modified surface.

Fine grains of laser modified substrate are thermally instable when subjected to high-temperature NiCrAlY splats. In previous work, the metastable phase formation in laser modified surface varies as a result of laser irradiance and residence time [10]. Lower irradiance at longer residence time or longer exposure time was necessary to allow surface melting to take place. A low heating rate and small undercooling along with longer exposure time produce martensite phase during processing. The pulse energy and residence time combination determine the surface heating rate and quench rate of undercooled austenite. Such treatment results in the formation of finer grains at the surface which enhances the strength of adhesion bond [11]. Thus, sample $L1$ has the highest interface bonding compared to sample $L2$ with lower laser peak power setup of 760 W and higher duty cycle setup of 36.1% .

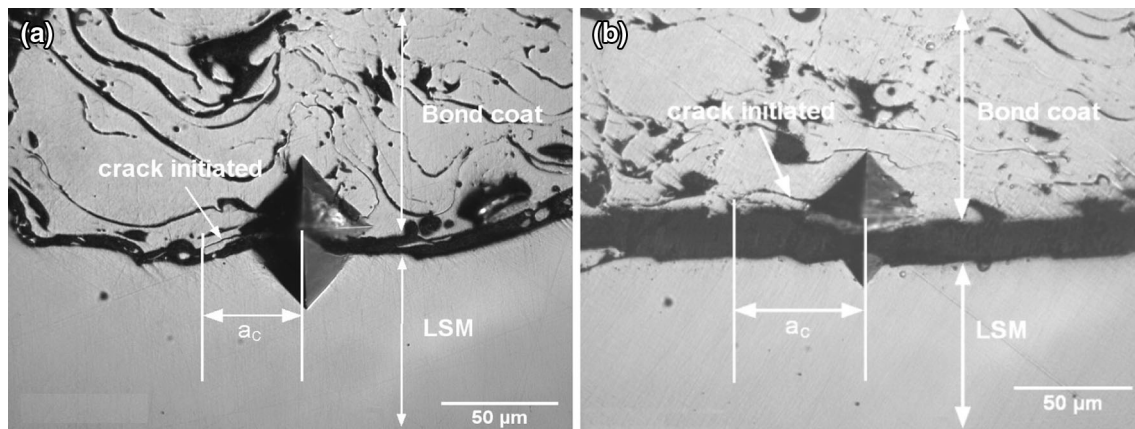


Fig. 3 Micrographs of **a** L1 and **b** L2 sample cross section with indentation mark at NiCrAlY coating/laser modified surface interface

Table 4 Average interfacial toughness ($\text{MPa m}^{1/2}$) of NiCrAlY coating on reference, L1 and L2 samples

Sample no.	Interfacial indentation force (kg)	Crack length, a_c (μm)	Interfacial toughness, K_C ($\text{MPa m}^{1/2}$)	Average interfacial toughness, K_{avg} ($\text{MPa m}^{1/2}$)
R1	0.5	71.20	2.00	2.15
R2	0.5	63.28	2.37	
R3	0.5	69.14	2.08	
L1a				
[i]	0.5	30.1	6.44	6.02
[ii]	0.5	33.2	5.58	
[iii]	0.5	31.4	6.05	
L1b				
[i]	1.0	50.2	5.99	6.96
[ii]	1.0	41.1	8.09	
[iii]	1.0	46.2	6.79	
L2a				
[i]	0.5	59.1	2.34	2.47
[ii]	0.5	57.6	2.44	
[iii]	0.5	54.7	2.63	
L2b				
[i]	1.0	80.2	2.97	3.46
[ii]	1.0	72.8	3.43	
[iii]	1.0	65.9	3.98	

Additionally, enhanced interfacial bonding between NiCrAlY coating and laser modified substrate of L1 sample was due to sinusoidal interface geometry as shown by micrographs in Fig. 4. NiCrAlY splats were entrapped within the slopes to produce mechanical keying or physical interlocking that allows interface bonding. The steep slopes produced by lower peak power of 760 W engaged more materials entrapment and thus better adhesion bonding by physically interlocking the coating–modified substrate interface. In Fig. 5, the gradual slope in L2 sample impeded

strong coating adhesion. Parallel with previous work, at higher power setting of 1515 W, surface roughness of modified surface ranged from 1.8 to 4.0 μm , whereas at lower power setting of 760 W, the surface roughness was between 5.0 and 6.5 μm [12].

3.2 Energy-dispersive X-ray spectroscopy (EDXS)

In L1 sample shown in Fig. 4a, three layers were observed along the cross-sectional depth, namely NiCrAlY coating, laser-modified substrate (LSM) and H13 substrate. EDXS analysis detected changes of nickel, chromium, aluminum, oxygen and iron element content along cross-sectional depth of bond coat (NiCrAlY) layer (points A–C), laser modified surface (LSM) layer (D) and substrate (E–F) as shown in Fig. 4b.

Based on Fig. 4b, elemental changes for L1 sample analyzed in coating layer from point A to point C indicate the presence of iron or Fe as high as 13.6 wt% and decreasing Ni and Cr content. Referred to Table 5, Ni decreased from its highest level of 64.6 wt% at point A to 50.6 wt% at point C. Cr was detected at the highest level of 21.5 wt% at point B and decreased to 17.5 wt% at point C. Varying Al content was observed in the coating layer at 2.8–9.5 wt%. At point C, metallography of the NiCrAlY revealed visible splat boundaries and small amount of internal porosity, where existence of oxygen in this region rapidly reacts with Al to form alumina, Al_2O_3 . This alumina was detected with O presence of 8.2 wt%. Presence of Al at 0.7 wt% with a higher Ni and Cr content at point D was detected relative to the H13 steel substrate. At point D, the chemical composition detected was 5.7 wt% Ni, 6.6 wt% Cr, 0.7 wt% Al and 83.8 wt% iron or Fe. From point E to point F, H13 steel substrate composed of 3.3 wt% Ni, 5.5–5.7 wt% Cr.

For L2 sample, there were 3 surface layers observed along the cross-sectional depth referred to Fig. 5a, and the

Fig. 4 Micrograph of sample L1 cross section **a** with NiCrAlY coating layer, laser-modified surface and substrate, and **b** close-up with six EDXS scan points along depth

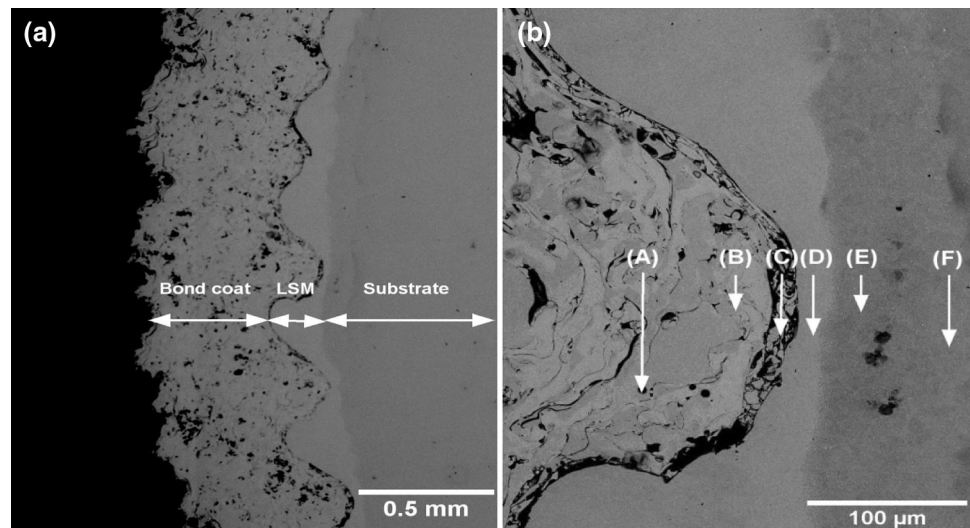


Fig. 5 Micrograph of sample L2 cross section **a** with NiCrAlY coating layer, laser-modified surface and substrate, and **b** close-up with six EDXS scan points along depth

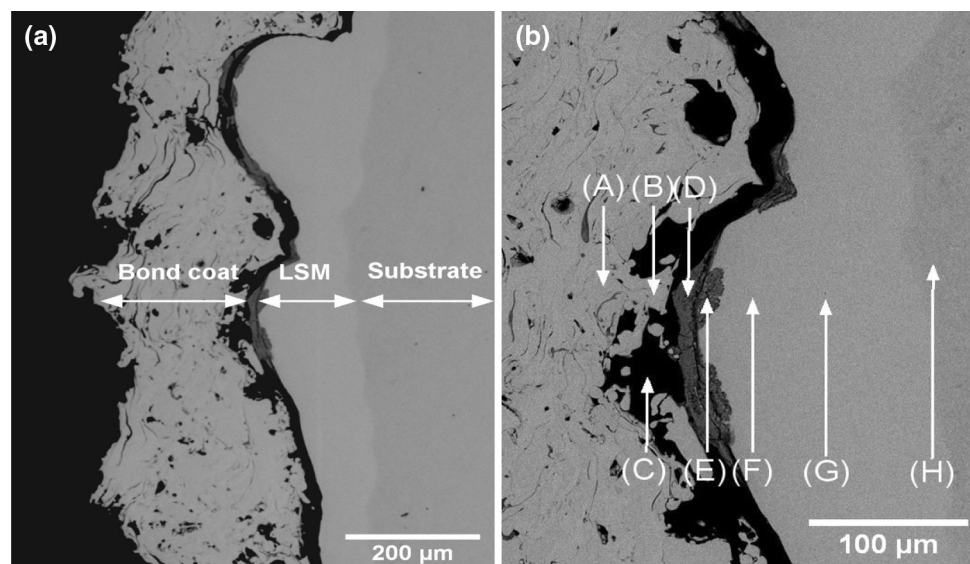


Table 5 Weight percentage (wt%) of element as a function of position from surface for sample L1

Position (wt%)	Ni	Cr	Al	Y	O	Fe
A	64.6	21.1	2.8	0	1.2	10.3
B	60.5	21.5	8.8	0.8	0	8.5
C	50.6	17.5	9.5	0.7	8.2	13.6
D	5.7	6.6	0.7	0	0	83.8
E	3.3	5.7	0	0	0	87.1
F	3.3	5.5	0	0	0	85

layers were bond coat, laser surface modified (LSM) and substrate layers. EDXS analysis detected changes of nickel, chromium, aluminum, oxygen and iron element content

along cross-sectional depth of bond coat (NiCrAlY) coating (points A and B), oxide layer (C), outer oxide layer (points D and E), laser modified surface layer (points F and G) and substrate (H) as shown in Fig. 5b.

Based on Fig. 5b, elemental changes analyzed in coating layer from point A to point B indicate the presence of iron as high as 5.8 wt% and decreasing Ni and Cr content. Referred to Table 6, Ni increased from its lowest level of 62.8 wt% at point A to 64.9 wt% at point B. Cr was detected at the lowest level of 19.4 wt% at point A and increased to 21.2 wt% at point B. Similar pattern was observed for Al content, which has lowest level of 8.8 wt% at point A and 8.9 wt% at point B. At point C, oxidation during APS spraying inspired O to react with Al on the coating surface to form voids and external oxide layer

Table 6 Weight percentage (wt%) of element as a function of position from surface for sample L2

Position (wt%)	Ni	Cr	Al	Y	O	Fe
A	62.8	19.4	8.8	0.5	2.8	5.8
B	64.9	21.2	8.9	1.5	3.4	0
C	31.6	11.4	3.7	1.2	16.8	32.9
D	7.1	3.4	0	0	26	61.6
E	5.3	11.9	0	0	21.6	55.4
F	3.2	6.6	0	0	0	86.9
G	0	5.9	0	0	0	90.3
H	1.9	5.1	0	0	0	86.5

along substrate–bond coat interface that produced alumina, Al_2O_3 . This alumina was detected with O presence of 16.8 wt%. At points D and E, rich Ni and Cr outer oxide layer were detected with O presence of 21.6–26 wt%. The chemical composition between points D and E was in the range of 7.1–5.3 wt% Ni, 3.4–11.9 wt% Cr and 0 wt% Al. Presence of higher Ni and Cr content at points F and G was detected relative to the H13 steel substrate. Between points F and G, the chemical composition detected was in the range of 3.2–0 wt% Ni, 6.6–5.9 wt% Cr and 86.9–90.3 wt% Fe. At point H, H13 steel substrate composed of 1.9 wt% Ni and 5.1 wt% Cr.

Presence of Fe in NiCrAlY coating indicates diffusion of Fe element from laser modified surface to the coating layer. During plasma spray process, molten NiCrAlY was deposited onto H13 substrate surface which was laser modified beforehand to produce fine grains at metastable phase [13]. The grain refinement in laser modified sample is thermally instable and changes when subjected to high temperature of 650 °C [14]. Therefore, atomic diffusion easily occurred in metastable phase surface as kinetics mechanisms were active during coating process and energy barriers to atomic motion easily overcome [15].

Higher Ni and Cr content found in laser modified surface suggests diffusion of these elements from NiCrAlY coating to the modified surface. During coating deposition, high temperature of NiCrAlY splats energized the modified substrate surface. The energized metastable phase in modified substrate caused grain migration in conjunction with atomic diffusion. Coating layers containing diffused atoms developed strong bonding which is comparable to diffusion coating method.

Coating of NiCrAlY involves high temperature when using plasma spray processing. Thermally grown oxide (TGO) scale starts to form by interaction with oxidizing atmosphere. Formation of alumina, Al_2O_3 , in the TGO layer results the changes of Al content in coating layer where Al_2O_3 was formed from the diffusion of Al to TGO layer and finally oxidized with O [16]. The occurrence of

rich Ni, Cr outer oxide layer at points D and E in sample L2 associates this process to zero local concentration of aluminum. High content of O implies local activity of oxygen to form other oxides as Ni and Cr oxides. Strawbridge et al. [17] accounted that tensile stress normal to the oxide–metal (Ni and Cr oxides) would develop that effect in decreasing coating adhesion.

4 Conclusion

Enhanced interfacial toughness was determined in laser modified substrate sample of L1. The interfacial bonding toughness was due to metastable phase presence in laser modified substrate, sinusoidal interfacial geometry and atomic diffusion mechanism between NiCrAlY coating and laser modified surface. The metastable phase in modified substrate induced Fe, Ni and Cr atomic diffusion occurrence in both coating and laser modified layers. These findings introduce enhancement of coating system by substrate surface modification for interfacial adhesion.

Acknowledgments The authors would like to acknowledge the Ministry of Education Malaysia under Fundamental Research Grant Scheme RDU 120105 and University Malaysia Pahang for supporting this research study.

References

1. G. Zhao, J. Zhao, *Rare Met.* **31**(4), 362–367 (2012)
2. T. Lertjirakul, Y. Boonyongmaneerat, P. Visuttipitukul, *Adv. Mater. Res.* **1025–1026**, 737–744 (2014)
3. S.N. Aqida, et al., *Key Eng. Mater.* **504** (2012)
4. G. Telasang et al., *Surf. Coat. Technol.* **261**, 69–78 (2015)
5. Y.Z. Liu et al., *Mater. Des.* **80**, 63–69 (2015)
6. F. Cao, B. Tryon, C.J. Torbet, T.M. Pollock, *Acta Mater.* **57**, 3885–3894 (2009)
7. T.M. Pollock, D.M. Lipkin, K.J. Hemker, *MRS Bull.* **37**, 923–931 (2012)
8. A.G. Evans, D.R. Mumm, J.W. Hutchinson, G.H. Meier, F.S. Pettit, *Prog. Mater. Sci.* **46**, 505–553 (2001)
9. D. Chicot, P. Demarecaux, J. Lesage, *Thin Solid Films* **283**, 151–157 (1996)
10. S.N. Aqida, S. Naher, D. Brabazon, *American Institute of Physics* **1353**, 1081 (2011)
11. S.N. Aqida, D. Brabazon, S. Naher, *Appl. Phys. A* **110**(3), 673–678 (2013)
12. S.N. Aqida, D. Brabazon, S. Naher, *American Institute of Physics* **1315**, 1371 (2011)
13. F. Fazliana, S. Naher, D. Brabazon, F. Calosso, M. Rosso, J. Mech. Eng. Sci. (JMES) **6**, 975–980 (2014)
14. K. Chang, M. Baben, D. Music, D. Lange, H. Bolvardi, J.M. Schneider, *Acta Mater.* **98**, 135–140 (2015)
15. D. Matejka, B. Benko, *Plasma Spraying of Metallic and Ceramic Materials*, (Wiley, Hoboken, 1989)
16. L. Čelko, V. Řičánková, L. Klakurková, T. Podrábský, E. Dvořáček, J. Švejcar, *Act. Phys. Pol. A* **120**(2), 336–339 (2011)
17. A. Strawbridge, H.E. Evans, C.B. Ponton, *Mater. Sci. Forum* **251–254**, 365 (1997)